Power losses in the screens of the symmetrical three phase high current busduct

Zygmunt Piątek, Tomasz Szczegielniak, Dariusz Kusiak
Czestochowa University of Technology
42-200 Częstochowa, ul. Brzeźnicka 60a,
e-mail: zygmunt.piatek@interia.pl, dariuszkusiak@wp.pl,
szczegielniakt@interia.pl

Design of the high current busducts on high currents and voltages causes necessity precise describing of electromagnetic, dynamic and thermal effects. Knowledge of the relations between electrodynamics and constructional parameters is necessary in the optimization construction process of the high current busducts. Information about distribution electromagnetic field and power losses is a base into analysis of electrodynamics and thermal effects in the high current busducts. In the paper using the Poynting theorem and Jolule-Lenz law the active and reactive power in the screens of the symmetrical high current busduct were determined. Into account were taken internal and external proximity effect.

1. Introduction

Following the development of thermal and hydroelectric power stations, at the beginning of the 30s, high current transmission lines with screened busducts connecting big generators with unit transformers began to be installed (Fig. 1). The contemporary solutions consist of transmission lines isolated with air at atmospheric pressure, with duty-rated voltage values reaching up to 36 kV and duty-rated current values reaching up to: 10 kA for hydroelectric power plants, 20 kA for thermal and nuclear plants whose duty-rated power values reach up to 900 MW, 31,5 kA for nuclear plants with power value of 1300 MW [1-9].

Fig. 1. Isolated phase busduct [5]

Today high current busducts are applied in many projects around the world when high-power transmission with high reliability and maximum availability is required. The size of the projects are constantly increasing: from typically some hundred meters system length to typically several kilometers [1-7].

The design of the busducts used for high currents and voltages causes a necessity of precise describing of electromagnetic, dynamic and thermal effects. Knowledge of the relations between electrodynamics and constructional parameters is necessary in the optimization construction process of the high current busducts [1-7].

Power losses depend on value of currents, but for the large cross-sectional dimensions of the phase conductor, even for industrial frequency, skin, external (Fig. 2) and internal (Fig. 3) proximity effect should be taken into account [6-9].

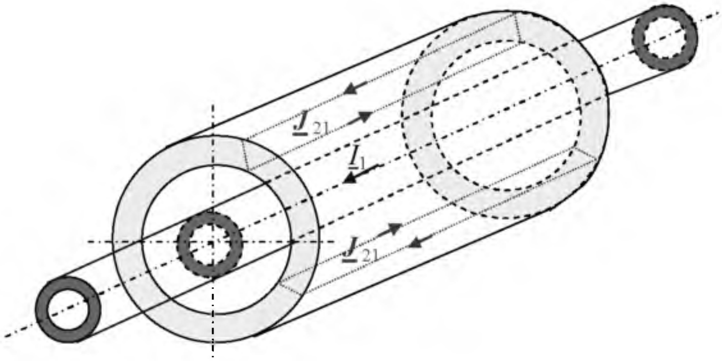

Fig. 2. Eddy currents induced in the screen by the magnetic field of the own current of the phase conductor

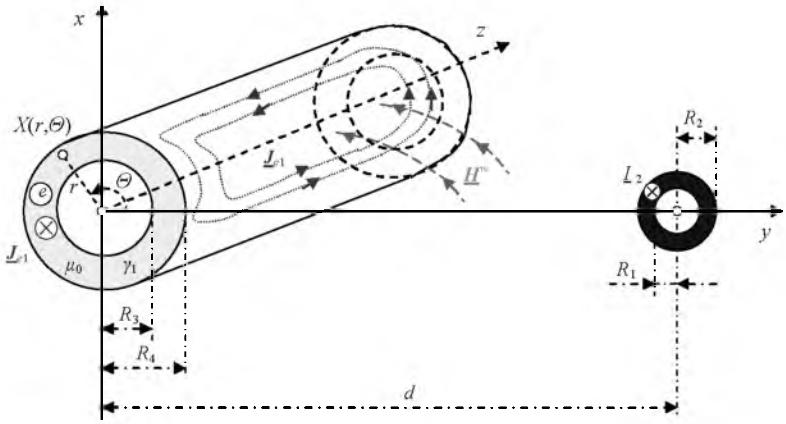

Fig. 3. Eddy currents induced in the screen by the magnetic field of the neighboring phase conductor

2. Electromagnetic field in the screens of the symmetrical three phase high current busduct

Let us consider the electromagnetic field in the screens of the symmetrical three phase high current busduct presented in the Fig. 4.

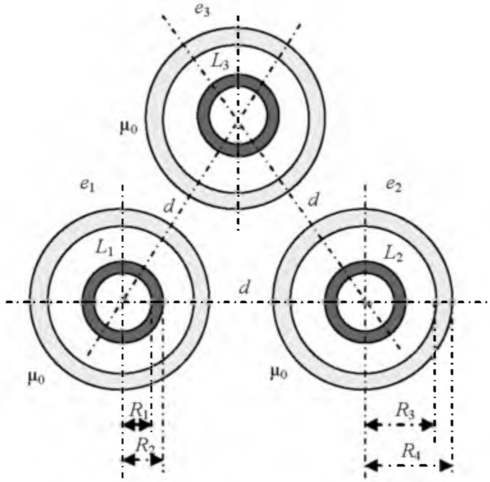

Fig. 4. Symmetrical three phase high current busduct

In the case of the symmetrical three phase high current busduct shown in figure 4, total density current $\underline{J}_{e1}(r,\Theta)$ in the first screen is a sum of densities of currents induced by each conductor

$$\underline{J}_{e1}(r,\Theta)=\underline{J}_{e11}(r,\Theta)+\underline{J}_{e12}(r,\Theta)+\underline{J}_{e13}(r,\Theta)=\underline{J}_{e11}(r,\Theta)+\underline{J}_{e123}(r,\Theta) \quad (1)$$

Total density current in the first screen $\underline{J}_{e1}(r,\Theta)$ depends on currents $\underline{I}_1$, $\underline{I}_2$, $\underline{I}_3$. If they form a symmetrical three of a three-phase system currents [6-9]:

$$\underline{I}_2=\exp[-\mathrm{j}\frac{2}{3}\pi]\underline{I}_1 \quad \text{and} \quad \underline{I}_3=\exp[\mathrm{j}\frac{2}{3}\pi]\underline{I}_1 \qquad (2)$$

then current density $\underline{J}_{e1}(r,\Theta)$ has a form

$$\underline{J}_{e11}(r)=\frac{\underline{\Gamma}_e\,\underline{I}_1}{2\pi R_3}\,\underline{j}_{e0}(r)=\frac{\underline{\Gamma}_e\,\underline{I}_1}{2\pi R_3}\,\frac{\underline{b}_0\,I_0(\underline{\Gamma}_e\,r)+\underline{c}_0\,K_0(\underline{\Gamma}_e\,r)}{\underline{d}_0} \qquad (3)$$

where

$$\underline{d}_0=I_1(\underline{\Gamma}_e R_4)\,K_1(\underline{\Gamma}_e R_3)-I_1(\underline{\Gamma}_e R_3)\,K_1(\underline{\Gamma}_e R_4) \quad \text{(3a)}$$

$$\underline{b}_0=\beta_e\,K_1(\underline{\Gamma}_e R_3)-K_1(\underline{\Gamma}_e R_4) \quad \text{(3b)}$$

$$\underline{c}_0 = \beta_e\, I_1(\underline{\Gamma}_e R_3) - I_1(\underline{\Gamma}_e R_4) \quad (3c)$$

$$\beta_e = \frac{R_3}{R_4} \;\; (0 \le \beta_e \le 1) \quad (3d)$$

and current density $\underline{J}_{e123}(r,\Theta)$ is defined by formula

$$\underline{J}_{e123}(r,\Theta) = \underline{J}_{e12}(r,\Theta) + \underline{J}_{e13}(r,\Theta) = -\frac{\underline{\Gamma}_e\, \underline{I}_1}{\pi R_4} \sum_{n=1}^{\infty} \underline{D}_n \left(\frac{R_4}{d}\right)^n \underline{f}_{ne}(r) \qquad (4)$$

where

$$\underline{D}_n = \exp\left[-\mathrm{j}\frac{2}{3}\pi\right]\cos n\Theta + \exp\left[\mathrm{j}\frac{2}{3}\pi\right]\cos n\left(\Theta - \frac{\pi}{3}\right) \qquad (4a)$$

and

$$\underline{f}_{ne}(r) = \frac{K_{n+1}(\underline{\Gamma}_e R_3)\, I_n(\underline{\Gamma}_e r) + I_{n+1}(\underline{\Gamma}_e R_3)\, K_n(\underline{\Gamma}_e r)}{I_{n-1}(\underline{\Gamma}_e R_4)\, K_{n+1}(\underline{\Gamma}_e R_3) - I_{n+1}(\underline{\Gamma}_e R_3)\, K_{n-1}(\underline{\Gamma}_e R_4)} \qquad (5)$$

In the above formulas $I_0(\underline{\Gamma}_e r)$, $K_0(\underline{\Gamma}_e r)$, $I_1(\underline{\Gamma}_e r)$, $K_1(\underline{\Gamma}_e r)$, $I_n(\underline{\Gamma}_e r)$, $K_n(\underline{\Gamma}_e r)$, $I_{n-1}(\underline{\Gamma}_e r)$, $K_{n-1}(\underline{\Gamma}_e r)$, $I_{n+1}(\underline{\Gamma}_e r)$ and $K_{n+1}(\underline{\Gamma}_e r)$ are modified Bessel's functions, 0, 1, *n*, *n*-1 and *n*+1 order, calculated for $r = R_3$ and $r = R_4$ [10], and the complex propagation constant of electromagnetic wave in the screen

$$\underline{\Gamma}_e = \sqrt{\mathrm{j}\,\omega\, \mu_0\, \gamma_e} = \sqrt{\omega\, \mu_0\, \gamma_e}\, \exp[\mathrm{j}\frac{\pi}{4}] = k_e + \mathrm{j}\, k_e \qquad (6)$$

in which attenuation constant

$$k = \sqrt{\frac{\omega \mu_0 \gamma_e}{2}} = \frac{1}{\delta} \qquad (7)$$

where δ is the electrical skin depth of the electromagnetic wave penetration into the conducting environment, ω is an angular frequency, γ_e means conductivity of the screen, and $\mu_0 = 4\pi\, 10^{-7}\ \mathrm{H \cdot m^{-1}}$ is magnetic permeability of the vacuum.

Total electric field in the first screen has a form

$$\underline{E}_{e1}(r,\Theta) = \underline{E}_{e11}(r) + \underline{E}_{e123}(r,\Theta) = \frac{\underline{\Gamma}_e\, \underline{I}_1}{2\pi\gamma_e R_3}\left[\underline{j}_{e0}(r) - 2\frac{R_3}{R_4}\sum_{n=1}^{\infty}\underline{D}_n \left(\frac{R_4}{d}\right)^n \underline{f}_{ne}(r)\right] \qquad (8)$$

Total magnetic field in the first screen has a form

$$\underline{\boldsymbol{H}}_{e1}(r,\Theta) = \underline{\boldsymbol{H}}_{e11}(r) + \underline{\boldsymbol{H}}_{e12}(r,\Theta) + \underline{\boldsymbol{H}}_{e13}(r,\Theta) = \mathbf{1}_r \underline{H}_{e1r}(r,\Theta) + \mathbf{1}_\Theta \underline{H}_{e1\Theta}(r,\Theta) \qquad (9)$$

where $\underline{\boldsymbol{H}}_{e11}(r) = \mathbf{1}_\Theta \underline{H}_{e11\Theta}(r)$ in which

$$\underline{H}_{\mathrm{e}11\Theta}(r)=\frac{\underline{I}}{2\pi R_3}\underline{h}_{\mathrm{e}0}(r)=\frac{\underline{I}}{2\pi R_3}\frac{\underline{b}_0\,I_1(\underline{\Gamma}_\mathrm{e}r)-\underline{c}_0\,K_1(\underline{\Gamma}_\mathrm{e}r)}{\underline{d}_0} \tag{10}$$

and $\underline{\boldsymbol{H}}_{e12}(r,\Theta)$, $\underline{\boldsymbol{H}}_{e13}(r,\Theta)$ are magnetic fields in the first screen created by currents $\underline{I}_2$ and $\underline{I}_3$.

The radial component

$$\underline{H}_{1r}(r,\Theta)=\underline{H}_{12r}(r,\Theta)+\underline{H}_{13r}(r,\Theta)=\underline{H}_{123r}(r,\Theta) \tag{11}$$

For the symmetrical three of a three-phase system currents (2) radial component of the magnetic field has a form

$$\underline{H}_{e123r}(r,\Theta)=\underline{H}_{e1r}(r,\Theta)=-\frac{\underline{I}_1}{\pi\,\underline{\Gamma}_\mathrm{e}\,R_4\,r}\sum_{n=1}^{\infty}\underline{F}_n\left(\frac{R_4}{d}\right)^n n\,\underline{f}_{ne}(r) \tag{12}$$

where

$$\underline{F}_n=\exp\left[-\mathrm{j}\frac{2}{3}\pi\right]\sin n\Theta+\exp\left[\mathrm{j}\frac{2}{3}\pi\right]\sin n\left(\Theta-\frac{\pi}{3}\right) \tag{12a}$$

Tangent component of the magnetic field in the first screen

$$\underline{H}_{e1\Theta}(r,\Theta)=\underline{H}_{e11\Theta}(r)+\underline{H}_{e12\Theta}(r,\Theta)+\underline{H}_{e13\Theta}(r,\Theta)=\underline{H}_{e11\Theta}(r)+\underline{H}_{e123\Theta}(r,\Theta) \tag{13}$$

while magnetic field $\underline{H}_{e11\Theta}(r)$ is defined by formula (10), but $\underline{H}_{e123\Theta}(r,\Theta)$ has a form

$$\underline{H}_{e123\Theta}(r,\Theta)=-\frac{\underline{I}_1}{\pi\,\underline{\Gamma}_\mathrm{e}R_4\,r}\sum_{n=1}^{\infty}\underline{D}_n\left(\frac{R_2}{d}\right)^n\left[-n\,\underline{f}_{ne}(r)+\underline{g}_{ne}(r)\right] \tag{14}$$

Hence the tangent component of the magnetic field in the first screen has a following form

$$\underline{H}_{e1\Theta}(r,\Theta)=\frac{\underline{I}_1}{2\pi R_3}\left\{\underline{h}_{e0}(r)-\frac{2R_3}{\underline{\Gamma}_\mathrm{e}R_4\,r}\sum_{n=1}^{\infty}\underline{D}_n\left(\frac{R_4}{d}\right)^n\left[-n\,\underline{f}_{ne}(r)+\underline{g}_{ne}(r)\right]\right\} \tag{15}$$

In the second screen total current density is defined by formula (1) in which current density $\underline{J}_{e22}(r)$ is defined by formula (3) in which current $\underline{I}_1$ should be replaced by $\underline{I}_2$. The same current density $\underline{J}_{e213}(r)$ has a form (4) in which current $\underline{I}_1$ should be replaced by $\underline{I}_2$, but constant $\underline{D}_n$ by

$$\underline{G}_n=(-1)^n\left\{\exp\left[\mathrm{j}\frac{2}{3}\pi\right]\cos n\Theta+\exp\left[-\mathrm{j}\frac{2}{3}\pi\right]\cos n\left(\Theta+\frac{\pi}{3}\right)\right\} \tag{16}$$

Total magnetic field in the second screen is defined by formula (9), where $\underline{\boldsymbol{H}}_{e22}(r) = \mathbf{1}_{\Theta}\underline{H}_{e22\Theta}(r)$ in which $\underline{H}_{e22\Theta}(r)$ is defined by formula (10) in which current $\underline{I}_1$ should be replaced by $\underline{I}_2$. Radial component of the magnetic field in the second screen is defined by formula (12) in which constant $\underline{F}_n$ should be replaced by

$$\underline{K}_n = (-1)^n \left\{ \exp\left[\mathrm{j}\frac{2}{3}\pi \right] \sin n\Theta + \exp\left[-\mathrm{j}\frac{2}{3}\pi \right] \sin n\left(\Theta + \frac{\pi}{3} \right) \right\} \tag{17}$$

Resultant tangent component of the magnetic field in the second screen $\underline{H}_{e2\Theta}(r,\Theta)$ has a form (15) in which current $\underline{I}_1$ should be replaced by $\underline{I}_2$, but constant $\underline{D}_n$ by $\underline{G}_n$.

In the third screen total current density is defined by formula (1) in which current density $\underline{J}_{e33}(r)$ is defined by formula (3) in which current $\underline{I}_1$ should be replaced by $\underline{I}_3$. The same current density $\underline{J}_{e312}(r)$ has a form (4) in which current $\underline{I}_1$ should be replaced by $\underline{I}_3$, but constant $\underline{D}_n$ by

$$\underline{M}_n = (-1)^n \exp\left[-\mathrm{j}\frac{2}{3}\pi \right] \cos n\left(\Theta - \frac{\pi}{3} \right) + \exp\left[\mathrm{j}\frac{2}{3}\pi \right] \cos n\left(\Theta + \frac{\pi}{3} \right) \tag{18}$$

Total magnetic field in the third screen is defined by formula (9), where $\underline{\boldsymbol{H}}_{e33}(r) = \mathbf{1}_{\Theta}\underline{H}_{e33\Theta}(r)$ in which $\underline{H}_{e33\Theta}(r)$ is defined by formula (10) in which current $\underline{I}_1$ should be replaced by $\underline{I}_3$. Radial component of the magnetic field in the third screen is defined by formula (12) in which constant $\underline{F}_n$ should be replaced by

$$\underline{N}_n = (-1)^n \exp\left[-\mathrm{j}\frac{2}{3}\pi \right] \sin n\left(\Theta - \frac{\pi}{3} \right) + \exp\left[\mathrm{j}\frac{2}{3}\pi \right] \sin n\left(\Theta + \frac{\pi}{3} \right) \tag{19}$$

Resultant tangent component of the magnetic field in the third screen $\underline{H}_{e3\Theta}(r,\Theta)$ has a form (15) in which current $\underline{I}_1$ should be replaced by $\underline{I}_3$, but constant $\underline{D}_n$ by $\underline{M}_n$.

3. Power losses in the screens of the symmetrical three phase high current busduct

Apparent power of the first screen is equal [7-9]

$$\underline{S}_{e1} = -\oint\!\!\!\oint_S \left[\underline{\boldsymbol{E}}_{e1}(r) \times \underline{\boldsymbol{H}}^*_{e1}(r) \right] \cdot \mathrm{d}\boldsymbol{S} = P_{e1} + \mathrm{j}\,Q_{e1} \tag{20}$$

from where

$$\underline{S}_{e1} = \underline{S}_{e0} + \underline{S}_{e123} \tag{21}$$

where

$$\underline{S}_{\mathrm{e}0} = \frac{\underline{\Gamma}_{\mathrm{e}}\, l\, I_1^{\,2}}{2\,\pi\,\gamma_{\mathrm{e}} R_3} \frac{\underline{b}_0\left[I_0(\underline{\Gamma}_{\mathrm{e}}R_4) - I_0(\underline{\Gamma}_{\mathrm{e}}R_3)\right] + \underline{c}_0\left[K_0(\underline{\Gamma}_{\mathrm{e}}R_4) - K_0(\underline{\Gamma}_{\mathrm{e}}R_3)\right]}{\underline{d}_0} \tag{21a}$$

and

$$\underline{S}_{\mathrm{e}123} = \frac{\mathrm{j} I_1^{\,2} l}{\pi^2 \gamma_e R_4^2} \sum_{n=1}^{\infty} \left(\int_0^{2\pi} D_n^2 \,\mathrm{d}\Theta \right) \left(\frac{R_4}{d} \right)^{2n} \begin{Bmatrix} \underline{f}_{ne}(R_4)\left[-n\,\underline{f}_{ne}^{\,*}(R_4) + \underline{g}_{ne}^{\,*}(R_4)\right] \\ -\underline{f}_{ne}(R_3)\left[-n\,\underline{f}_{ne}^{\,*}(R_3) + \underline{g}_{ne}^{\,*}(R_3)\right] \end{Bmatrix} \tag{21b}$$

In the formula (21) we can not isolate the real part (as an active power) and the imaginary part (as a reactive power). It is impossible on account of the complex propagation constant and complex modified Bessel's functions. Therefore the active power will be calculated from formula [7-9]

$$P_{e1} = \iiint_V \frac{1}{\gamma_e} \underline{J}_{\mathrm{e}1}(r,\Theta)\, \underline{J}_{\mathrm{e}1}^{*}(r,\Theta)\,\mathrm{d}V = \frac{1}{\gamma_e} \int_0^{l} \int_0^{2\pi} \int_{R_3}^{R_4} \underline{J}_{\mathrm{e}1}(r,\Theta)\, \underline{J}_{\mathrm{e}1}^{*}(r,\Theta)\, r\,\mathrm{d}r\,\mathrm{d}\Theta\,\mathrm{d}z \tag{22}$$

From the formula (22) we get

$$P_{e1} = P_{e0} + P_{e123} \tag{23}$$

where

$$P_{\mathrm{e}0} = \frac{\underline{\Gamma}_{\mathrm{e}}^{*}\, l\, I_1^{\,2}}{4\,\pi\,\gamma_{\mathrm{e}}\,\beta_{\mathrm{e}}^2\, R_4} \frac{\underline{a}_0}{\underline{d}_0\,\underline{d}_0^{*}} \tag{23a}$$

and

$$P_{e123} = \frac{\underline{\Gamma}_e^{\,*}\, l\, I_1^2}{2\,\pi^2\,\gamma\,R_4} \sum_{n=1}^{\infty} \left(\int_0^{2\pi} D_n^2 \,\mathrm{d}\Theta \right) \left(\frac{R_4}{d} \right)^{2n} \frac{\underline{a}_{ne}}{\underline{b}_{ne}\,\underline{b}_{ne}^{*}} \tag{23b}$$

where

$$\begin{aligned} \underline{a}_0 = {} & \underline{b}_0\,\underline{b}_0^{*} \begin{Bmatrix} I_0^{*}(\underline{\Gamma}_{\mathrm{e}}R_4) I_1(\underline{\Gamma}_{\mathrm{e}}R_4) + \mathrm{j}\, I_0(\underline{\Gamma}_{\mathrm{e}}R_4) I_1^{*}(\underline{\Gamma}_{\mathrm{e}}R_4) - \\ -\beta_{\mathrm{e}}\left[I_0^{*}(\underline{\Gamma}_{\mathrm{e}}R_3) I_1(\underline{\Gamma}_{\mathrm{e}}R_3) + \mathrm{j}\, I_0(\underline{\Gamma}_{\mathrm{e}}R_3) I_1^{*}(\underline{\Gamma}_{\mathrm{e}}R_3)\right] \end{Bmatrix} - \\ & -\underline{c}_0\,\underline{c}_0^{*} \begin{Bmatrix} K_0^{*}(\underline{\Gamma}_{\mathrm{e}}R_4) K_1(\underline{\Gamma}_{\mathrm{e}}R_4) + \mathrm{j}\, K_0(\underline{\Gamma}_{\mathrm{e}}R_4) K_1^{*}(\underline{\Gamma}_{\mathrm{e}}R_4) - \\ -\beta_{\mathrm{e}}\left[K_0^{*}(\underline{\Gamma}_{\mathrm{e}}R_3) K_1(\underline{\Gamma}_{\mathrm{e}}R_3) + \mathrm{j}\, K_0(\underline{\Gamma}_{\mathrm{e}}R_3) K_1^{*}(\underline{\Gamma}_{\mathrm{e}}R_3)\right] \end{Bmatrix} - \\ & -\underline{c}_0\,\underline{b}_0^{*} \begin{Bmatrix} I_0^{*}(\underline{\Gamma}_{\mathrm{e}}R_4) K_1(\underline{\Gamma}_{\mathrm{e}}R_4) - \mathrm{j}\, K_0(\underline{\Gamma}_{\mathrm{e}}R_4) I_1^{*}(\underline{\Gamma}_{\mathrm{e}}R_4) - \\ -\beta_{\mathrm{e}}\left[I_0^{*}(\underline{\Gamma}_{\mathrm{e}}R_3) K_1(\underline{\Gamma}_{\mathrm{e}}R_3) - \mathrm{j}\, K_0(\underline{\Gamma}_{\mathrm{e}}R_3) I_1^{*}(\underline{\Gamma}_{\mathrm{e}}R_3)\right] \end{Bmatrix} + \\ & +\underline{b}_0\,\underline{c}_0^{*} \begin{Bmatrix} I_1(\underline{\Gamma}_{\mathrm{e}}R_4) K_0^{*}(\underline{\Gamma}_{\mathrm{e}}R_4) - \mathrm{j}\, I_0(\underline{\Gamma}_{\mathrm{e}}R_4) K_1^{*}(\underline{\Gamma}_{\mathrm{e}}R_4) - \\ -\beta_{\mathrm{e}}\left[I_1(\underline{\Gamma}_{\mathrm{e}}R_3) K_0^{*}(\underline{\Gamma}_{\mathrm{e}}R_3) - \mathrm{j}\, I_0(\underline{\Gamma}_{\mathrm{e}}R_3) K_1^{*}(\underline{\Gamma}_{\mathrm{e}}R_3)\right] \end{Bmatrix} \end{aligned} \tag{23c}$$

$$\begin{aligned}\underline{a}_{\mathrm{ne}} = {} & I_{n+1}(\underline{\Gamma}_{\mathrm{e}}R_4)\,K_{n+1}(\underline{\Gamma}_{\mathrm{e}}R_3)\left[I^*_{n+1}(\underline{\Gamma}_{\mathrm{e}}R_3)\,K^*_n(\underline{\Gamma}_{\mathrm{e}}R_4) + I^*_n(\underline{\Gamma}_{\mathrm{e}}R_4)\,K^*_{n+1}(\underline{\Gamma}_{\mathrm{e}}R_3)\right] + \\ & + \mathrm{j}\,I_n(\underline{\Gamma}_{\mathrm{e}}R_4)\,K_{n+1}(\underline{\Gamma}_{\mathrm{e}}R_3)\left[I^*_{n+1}(\underline{\Gamma}_{\mathrm{e}}R_4)\,K^*_{n+1}(\underline{\Gamma}_{\mathrm{e}}R_3) - I^*_{n+1}(\underline{\Gamma}_{\mathrm{e}}R_3)\,K^*_{n+1}(\underline{\Gamma}_{\mathrm{e}}R_4)\right] - \\ & - I_{n+1}(\underline{\Gamma}_{\mathrm{e}}R_3)\begin{Bmatrix} K^*_{n+1}(\underline{\Gamma}_{\mathrm{e}}R_3)\left[I^*_n(\underline{\Gamma}_{\mathrm{e}}R_4)\,K_{n+1}(\underline{\Gamma}_{\mathrm{e}}R_4) - \mathrm{j}\,I^*_{n+1}(\underline{\Gamma}_{\mathrm{e}}R_4)\,K_n(\underline{\Gamma}_{\mathrm{e}}R_4)\right] + \\ + I^*_{n+1}(\underline{\Gamma}_{\mathrm{e}}R_3)\left[K^*_n(\underline{\Gamma}_{\mathrm{e}}R_4)\,K_{n+1}(\underline{\Gamma}_{\mathrm{e}}R_4) + \mathrm{j}\,K^*_{n+1}(\underline{\Gamma}_{\mathrm{e}}R_4)\,K_n(\underline{\Gamma}_{\mathrm{e}}R_4)\right]\end{Bmatrix}\end{aligned} \tag{23d}$$

$$\underline{b}_{ne} = I_{n-1}(\underline{\Gamma}_{\mathrm{e}}R_4)\,K_{n+1}(\underline{\Gamma}_{\mathrm{e}}R_4) - I_{n+1}(\underline{\Gamma}_{\mathrm{e}}R_4)\,K_{n-1}(\underline{\Gamma}_{\mathrm{e}}R_4) \tag{23e}$$

$$\underline{b}^*_{ne} = I^*_{n-1}(\underline{\Gamma}_{\mathrm{e}}R_4)\,K^*_{n+1}(\underline{\Gamma}_{\mathrm{e}}R_3) - I^*_{n+1}(\underline{\Gamma}_{\mathrm{e}}R_3)\,K^*_{n-1}(\underline{\Gamma}_{\mathrm{e}}R_4) \tag{23f}$$

If we introduce the reference active power [7-9]

$$P_{0\mathrm{ew}} = \frac{l\,I_1^2}{\pi\,\gamma_{\mathrm{e}}\,(R_4^2 - R_3^2)} \tag{24}$$

then the relative active power in the first screen has a form

$$k^{(P)}_{\mathrm{e}1} = \frac{P_{\mathrm{e}0} + P_{e123}}{P_{0\mathrm{cw}}} \tag{25}$$

Dependence of the coefficient (25) on parameter α_e for different values of the relative walls thickness β_e of the first screen and of relative distance between conductors λ_{e} is presented in the Fig. 5 (where $\alpha_e = k_e R_4$, $\lambda_e = \dfrac{d}{R_3}$).

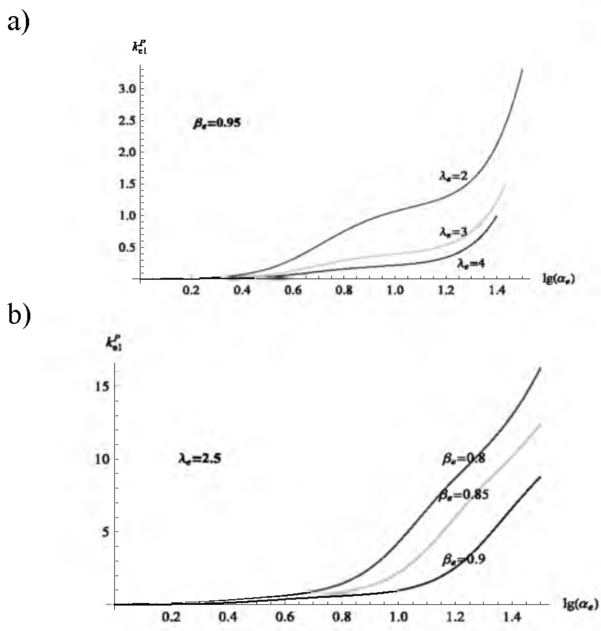

Fig. 5. Dependence of the relative active power in the first screen on parameter α_{e}:
a) for constant value of the parameter β_{e}, b) for constant of the parameter λ_{e}

The reactive power emitted on internal inductance of the first screen, we calculate from (20), thus

$$\underline{Q}_{e1} = \underline{Q}_{e0} + \underline{Q}_{e123} \tag{26}$$

where

$$\underline{Q}_{e0} = -\mathrm{j}\frac{l\, I^2}{2\,\pi\,\gamma_e\, R_3\, \underline{d}_0}\left\{\underline{\Gamma}_e\left[\begin{matrix}\underline{b}_0\left(I_0(\underline{\Gamma}_e R_4) - I_0(\underline{\Gamma}_e R_3)\right) + \\ + \underline{c}_0\left(K_0(\underline{\Gamma}_e R_4) - K_0(\underline{\Gamma}_e R_3)\right)\end{matrix}\right] - \frac{\underline{\Gamma}_e^*\, \underline{a}_0}{2\,\beta_e\, \underline{d}_0^*}\right\} \tag{26a}$$

and

$$\underline{Q}_{e123} = \frac{l\, I_1^2}{\pi^2\, \gamma\, R_4^{\ 2}} \sum_{n=1}^{\infty}\left(\int_0^{2\pi} D_n^2\, \mathrm{d}\Theta\right)\left(\frac{R_4}{d}\right)^{2n} \times \left\{\begin{matrix} n\left[\underline{f}_n(R_3)\,\underline{f}_n^*(R_3) - \underline{f}_n(R_4)\,\underline{f}_n^*(R_4)\right] + \\ \underline{f}_n(R_4)\,\underline{g}_n^*(R_4) - \underline{f}_n(R_3)\,\underline{g}_n^*(R_3) + \\ + \mathrm{j}\dfrac{\underline{\Gamma}_e^{\ *}\, R_4}{2}\dfrac{\underline{a}_{ne}}{\underline{b}_{ne}\, \underline{b}_{ne}^*} \end{matrix}\right\} \tag{26b}$$

If we introduce the reference reactive power [7-9]

$$\underline{Q}_{0ew} = X_{0ew}\, I_1^{\ 2} = \omega\frac{\mu_0\, l}{2\,\pi}\left[\frac{R_3^4}{\left(R_4^2 - R_3^2\right)^2}\ln\frac{R_4}{R_3} - \frac{1}{4}\frac{3R_3^2 - R_4^2}{R_4^2 - R_3^2}\right] I_1^2 \tag{27}$$

then the relative reactive power of the first screen has a form

$$k_{e1}^{(Q)} = \frac{\underline{Q}_{e0} + \underline{Q}_{e123}}{\underline{Q}_{0ew}} \tag{28}$$

Dependence of the coefficient (28) on parameter α_e for different values of the relative walls thickness β_e of the first conductor and of relative distance between conductors λ_e is presented in the Fig. 6.

In the same way we can calculated power losses in the second and third screen. Besides if we take into account that

$$\int_0^{2\pi} G_n^2\, \mathrm{d}\Theta = \int_0^{2\pi} M_n^2\, \mathrm{d}\Theta = \int_0^{2\pi} D_n^2\, \mathrm{d}\Theta \tag{29}$$

then

$$k_{e2}^{(P)} = \frac{P_2}{P_{0ew}} = k_{e3}^{(P)} = \frac{P_3}{P_{0ew}} = k_{e1}^{(P)} \tag{30}$$

and

$$k_{e2}^{(Q)} = \frac{\underline{Q}_2}{\underline{Q}_{0ew}} = k_{e3}^{(Q)} = \frac{\underline{Q}_3}{\underline{Q}_{0ew}} = k_{e1}^{(Q)} \tag{31}$$

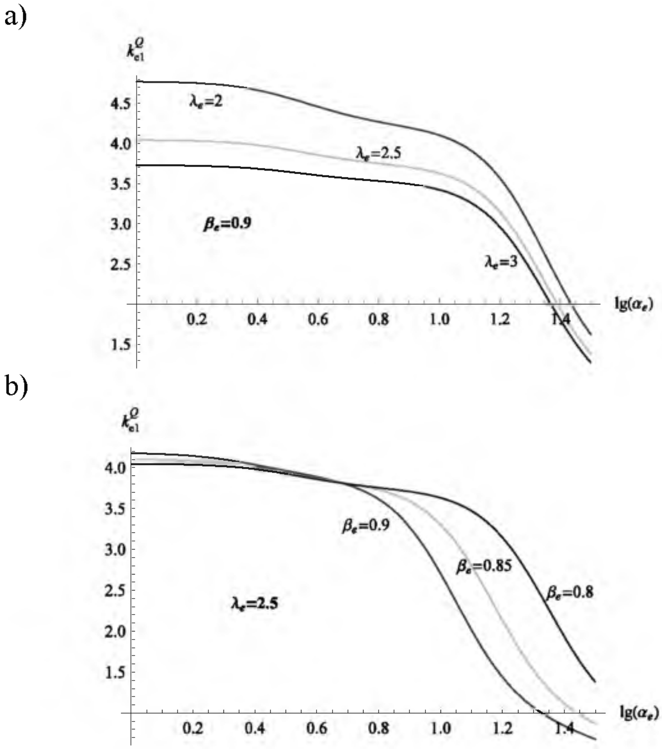

Fig. 6. Dependence of the relative reactive power of the first screen on parameter α_e:
a) for constant value of the parameter β_e, b) for constant of the parameter λ_e

4. Conclusions

In produced high current busducts, for industrial frequency value of parameter α_e is included from 5 to 20. It means that active power in the screens of the symmetrical three phase high current busduct can be ten times bigger than the active power calculated without taking into account proximity effect (Fig. 5).

Similarly, reactive power connected with internal inductance of the screen can be five times bigger than the reactive power calculated without taking into account proximity effect (Fig. 6).

Proximity effect depends on geometrical and physical parameters of the symmetrical high current busduct.

We should add that the total reactive power emitted in the screens of the symmetrical three phase high current busduct is a sum of the determined in the paper the reactive power connected with internal inductances of the screens and the reactive power connected with external and mutual inductances of the screens.

References

[1] Nawrowski R.: Tory wielkoprądowe izolowane powietrzem lub SF_6. Wyd. Pol. Poznańskiej, Poznań 1998.
[2] Piątek Z.: Impedances of high-current busducts. Wyd. Pol. Częst., Czestochowa 2008.
[3] CIGRE Brochure No 218.: *Gas Insulated Transmission Lines (GIL)*. WG 23/21/33-15, CIGRE, Paris, 2003.
[4] Koch H.: *Gas-Insulated Transmission Line (GIL)*. John Wiley & Sons, 2012.
[5] Holduct – Z. H. Ltd. Polska.: *Szynoprzewody trójfazowe okrągłe*. [Online]. Available: http://www.holduct.com.pl/index.php?menu=p2
[6] Kusiak D.: Pole Magnetyczne Dwu i Trójbiegunowych Torów Wielkoprądowych, Praca Doktorska, Częstochowa 2008.
[7] Szczegielniak T.: Straty mocy w nieekranowanych i ekranowanych rurowych torach wielkoprądowych, Praca Doktorska, Gliwice, 2011
[8] Szczegielniak T., Piątek Z., Kusiak D.: Straty mocy symetrycznego trójfazowego toru wielkoprądowego, Warsztaty Doktoranckie. Krynica-Zdrój, 2009.
[9] Szczegielniak T., Piątek Z., Kusiak D.: Straty mocy w ekranie trójfazowego symetrycznego toru wielkoprądowego, Warsztaty Doktoranckie, Lublin, 2010.
[10] Mc Lachlan N.W.: Funkcje Bessela dla inżynierów. PWN, Warszawa 1964.